IASS SYMPOSIUM 91

PROCEEDINGS OF THE INTERNATIONAL IASS SYMPOSIUM
2-6 SEPTEMBER 1991 · COPENHAGEN · DENMARK

Spatial Structures at the Turn of the Millennium

EDITORS TURE WESTER
STEFAN J. MEDWADOWSKI
IB MOGENSEN

KUNSTAKADEMIETS FORLAG ARKITEKTSKOLEN

VOLUME
I
Projects
and
Project Studies

The New Suspended Roof for the Olympic Stadium in Rome

M. MAJOWIECKI, University of Bologna, Italy

ABSTRACT

The actual stadium originally built for the 1960 Olympic Games, is now almost completely reconstructed. The grandstands have been substituted with new pre-fabricated prestressed concrete elements, increasing the total occupancy of 85000 spectators.
From the structural point of view the most impressive part of the stadium is the roofing structural system. Principally due to the existing boundary conditions the designers adopted an innovative design for the roofing of a football stadium. The system is formed mainly of: a radial distribution of cable trusses; an inner tension cable ring; a PTFE (Poly Tetra Fluoro Ethilene) membrane covering system.

Design criteria

The cable roofing system, used to cover the new Olympic stadium in Rome, is formed mainly of:

- a radial distribution of cable trusses;
- a polycentric inner tension cable ring;
- an outer anchorage system consisting of a space framed, reticular, polycentric ring.

Cable Trusses

The cable trusses, consisting of load-bearing cables, stabilizing cables and a connecting system of vertical, almost parallel cables, are distributed in a radial direction from centres C_1 and C_2 of the homothetic polycentric curves from which all the geometry of the stadium is generated (fig. 1).
In fig. 1 we can see that the cable trusses corresponding to alignements 1-5, symmetrical about x and y, are generated with a constant central angle of approximately 2°.31′. The structures aligned with cables 6-15 have generating angles which vary from 2°.26′ to 6°.87′, while from 15 to 20 the angle is constant at approximately 7°.6′.
The cable trusses are variously sized, and form two groups, depending on their state of stress and deformation. The main geometrical and mechanical features of the cable truss system are explained afterwards.
All of the cables are of a full-lock and/or open spiral type and are galvanized (class B). The main wires have an elementary strength of 1600 N/mm². The radial cable truss is combined with a secondary frame which supports the roof covering: girdes supported by a simple bearing system are suspended at the same leves as the stabilizing cables, forming a reticular truss. The roof covering, which is supported by and fastened to the extrados of the secondary girders, is made of a fiberglass membrane coated with PTFE (Teflon).

Polycentric inner ring

The inner ring, whose main function is to balance horizontal stresses transmitted by the radial trusses within a closed local system, is geometrically shown on the plan as two arcs with radii of 165.89 and 52.69 m respectively. The ring consists of 12 spiral, galvanized, full-lock coil cables, Ø 87 mm, arranged on a horizontal plane at a height of +29 m, and positioned so that, if viewed in cross-section, their barycentre points form a circle with an approximately 1 m diameter. The aim of the structure is to allow for practical connection with the radial cable trusses.

Outer anchorage ring

The load bearing and stabilizing cables are anchored around the outside to a space framed reticular ring, appearing as a polycentric circle on the plan with maximum external dimensions of 307.94 m for the larger diameter, and 237.28 m for the smaller one.
The ring has a triangular section, composing an upper chord made of tubular steel Fe 510 C with a 1400 mm diameter and thickness of 70-60 mm, positioned at a heigh of +36.49 m, and of two lower joists at +23.99 m and 25.89 m, made of tubular steel with a 1000 mm diameter and thickness of 16-18 mm. The overall dimensions of the triangle, measured along the axes, are 10.50 m along the base and 12.50 m, in height.

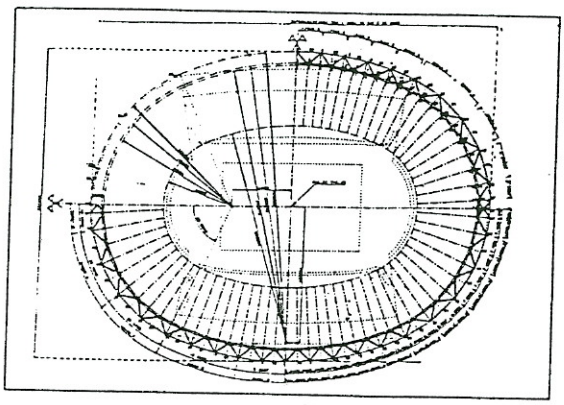

Fig. 1. Plan view of the structural axes layout with indication of the parameters from which the geometry of the whole structural system is generated.

The faces of the ring are reticulated by shafts (uprights and diagonal braces). The braces and uprights are made of tubes with a 609.6÷409.8 mm diameter and thickness of 10 and 8 mm respectively.
The generating radii on the plan are:

$$R_1 = 212 \text{ m}, \quad R_2 = 222.60 \text{ m},$$
$$R_3 = 98.90 \text{ m}, \quad R_4 = 109.40 \text{ m}.$$

Geometric mechanical model: the "0" state

The geometric model for a quarter of the structure was attained, using the structure's axes of symmetry, by means of the classic "0" state research method which is typically employed for cable trusses. After setting a certain prestress level on a group of truss member - whose topology is shown in fig. 2, preliminary research into the geometric-stress configuration was carried out, using the equilibrium condition of each inner joint, according to the following mathematical model:

$$\Sigma_i \vec{S}^{\circ}_{ki} + \vec{P}^{\circ}_{k} = 0$$

where:

$\vec{S}^{\circ}_{ki}$ = force vector in generic element ki in the "0" State

$\vec{P}^{\circ}_{k}$ = load vector applied to joint k in the "0" State.

Summation is extended to all of the elements joining K.
The final geometric configuration is depicted in figs. 3 and 4.
The geometric and mechanical features of the cable trusses forming a quarter of the ring

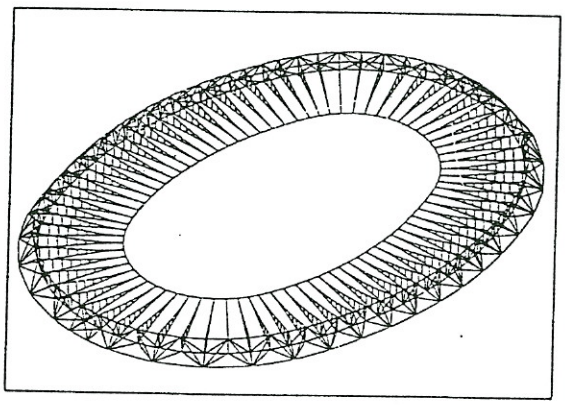

Fig. 2. Axonometric view of the geometric-mathematical model used for static and dynamic analysis of the roof's structural system.

are expressed in Table 1.
For symmetrical load combinations, a geometric model of a quarter of the structure (joints and elements) is considered.
For asymmetrical combination, a half of the structures is considered (with symmetry about the x and y axes).

Variations in state: mathematical model

Statical analysis

The state of stress in the cable truss, as a result of the various phases of static load considered, is analyzed using the "TENSO" program which works out the equivalent joint-element mesh by means of the equilibrium method, using the following condensed formula:

$$[K].\{\delta_k\}^r = \{P_k\} - \{P_k\}^{r-1}$$

where:

Table 1. List of dimensions of the cable system

Position		Ø mm	A (cm^2)	Cable L (m)	No. pieces	p (weight) (KN/m)	P_{tot} weight (KN)	Cable terminal
L-bearing	1÷10	64	27.50	55.20	38	0.23	48.2	F+R
L-bearing	11÷20	87	52.11	55.20	40	0.43	96.0	F+R
L-Stab.	1÷10	47	14.77	52.80	38	0.12	24.7	F+R
L-Stab.	11÷20	74	37.91	52.80	40	0.31	67.1	F+R
Ring		N*12-87	625	116.50	4	522	243.2	F+R
Hangers		2019	3.94	mean 4.00	1248	4	19.9	F+R

F = Fixed; R = Adjustable; P_{tot} = 5000 KN

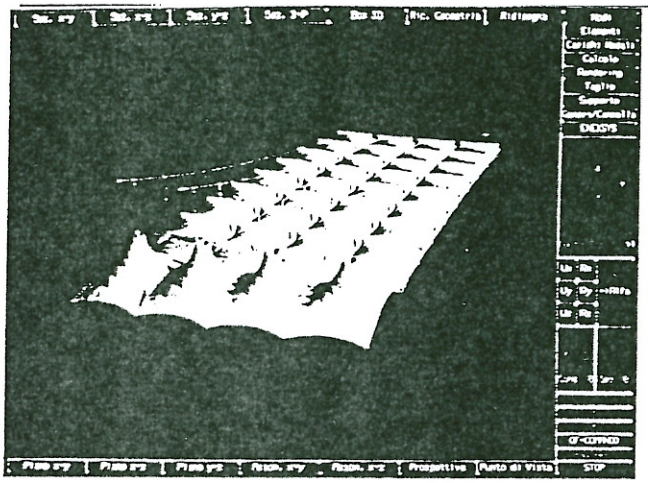

Fig. 3. Interactive sequences on the project (CAD: perspective view of 4 radial elements.

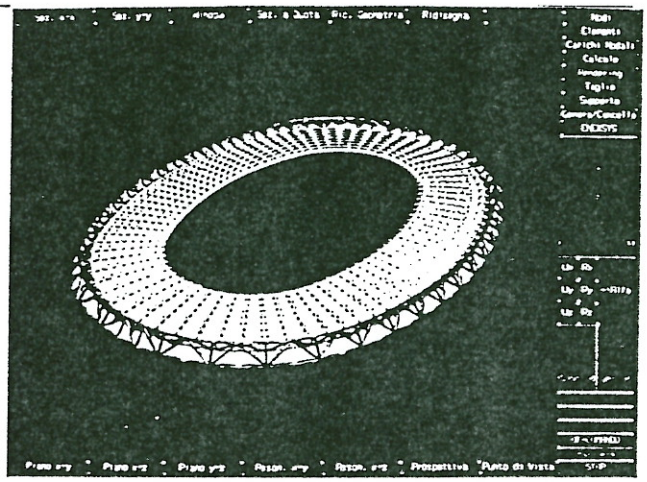

Fig. 4. General perspective view of the roofing system.

$[K]$ = global stiffness matrix ($[K] = [K_g] + [K_e]$);

$\{\delta_k\}^r$ = vectors of displacement at the r-iterative step;

$\{P_k\}$ = load applied to joint k;

$\{P_k\}^{r-1}$ = dummy load of nonlinear terms.

The numerical processes used to solve the system of nonlinear equations deriving from assembly of the elementary matrices is of a semi-incremental type where loads and material nonlinearity are concerned, and of an iterative type where geometrical nonlinearity is concerned. The cable system does not, by definition, allow for a state of compressive stress ($S < 0$). Each time that a load increment is made, the program checks the stresses on each element, and if $Skj < 0$, is removed and the local tangent stiffness matrix is accordingly changed.

Structural interaction. The sub-structuring method

Where elastic and non elastic interaction between the cable system and anchorage structures (reticulated ring) is concerned, the sub-structuring solution method has been adopted.

This method makes it possible to separately solve the two interacting structural systems. Let's consider that sub-structures I (cable system) and II (anchorage structure) are linked together in the group of B points (anchorage joints). By separating the displacements, we obtain the following equation:

$$\begin{bmatrix} K_{AA} & K_{AB} & \cdot & 0 \\ K_{AB}^T & K_{BB} & \cdot & G_B \\ \cdots & \cdots & \cdots & \cdots \\ 0 & -G_B^T & \cdot & F \end{bmatrix} \begin{bmatrix} \delta_A \\ \delta_B \\ \cdots \\ X \end{bmatrix} = \begin{bmatrix} P_A \\ P_B \\ \cdots \\ \delta \end{bmatrix}$$

where:

$[K]$ = stiffness matrix of sub-structure I in relation to type A (inner) and type B boundary joints;

$[F]$ = flexibility matrix of sub-structure II;

$[G]$ = coupling matrix between I and II;

δ_A, δ_B = vectors of displacement in I;

X = indeterminate or boundary forces;

P_A, P_B = load terms in I;

δ = displacement terms in II.

The solution in terms of displacement (equilibrium method) may be attained by considering:

$$\begin{bmatrix} K_{AA} & K_{AB} \\ K_{AB}^T & K_{BB} \end{bmatrix} \begin{bmatrix} \delta_A \\ \delta_B \end{bmatrix} = \begin{bmatrix} P_A \\ P_B^* \end{bmatrix}$$

with:

$$K^*_{BB} = K_{BB} + G_B F^{-1} G^T_B$$

and

$$P^*_B = P_B - G_B - G_B F^{-1} \delta$$

where the stiffness matrices and load vector are to be interpreted respectively as stiffness matrix and load vector, transformed by the effect of the displacements of type B joints at I and II. This procedure is equivalent to the static condensation of sub-structure II.
Some results from the geometrical non linear analysis of main loading combinations are illustrated in figs 5 and 6.

Random dynamic analysis in the frequency domain

In order to carry out a complete check of the structures' dynamic characteristics, a linear modal random dynamic analysis in the frequency domain was devised.
This dynamic analysis method involves determination of the power spectral density of the fluctuating part of the wind at the height of the roofing in question.
According to the ESDU spectrum, we have:

$$S_v(n) = 30.85\ V/[1+337500\ (n/V)^2]^{5/6}$$

where: n = frequency.

The expression of correlated spectral density (function of spatial correlation) is:

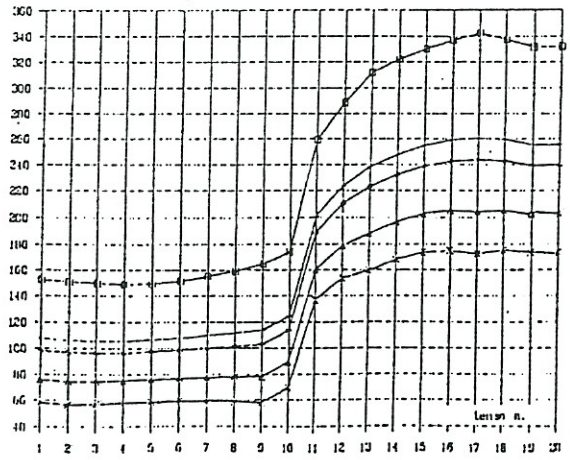

Fig. 5. Force distribution on carrying cables under different load combinations.

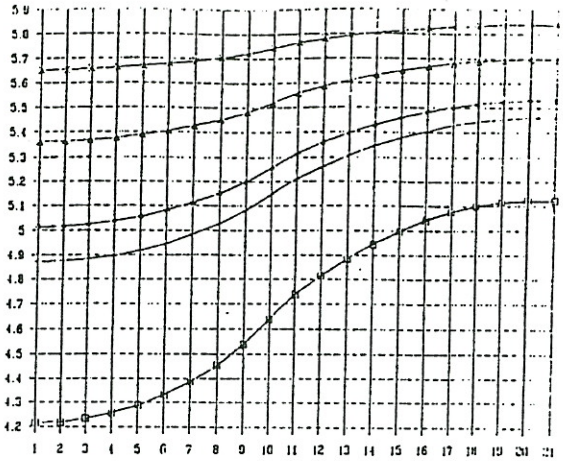

Fig. 6. Deformed geometry of the inner ring between main axis.

$$S_{vj}(P_1, P_2, n) = S_v(20, n)\ \mathrm{Coh}\ (P_1, P_2, n)$$

The power spectral density of dynamic pressure is attained by:

$$S_{pj}(P_1, P_2, n) = C^2\ \rho^2\ V^2\ S_v(P_1, P_2, n)$$

The PSD, in terms of nodal forces, is expressed by:

$$S_{fj}(P_1, P_2, n) = S_p\ (P_1, P_2, n)\ A_j^2$$

The Sfj matrix is shown to be an NxN matrix for all frequencies considered, with Aj = area of influence of joint j.

Modal power spectral density

By using modal analysis and considering the first **m** vibration modes, we have:

$$[S\ \emptyset(n)] = [\emptyset]^T\ [S_f][\emptyset]$$

where the [Ø] columns contain the **n** vibration modes (fig. 7) considered: for each joint, the vertical components of the N joints of the structural system.
The dimensions of the [SØ(n)] are mxm.

Power spectral density of the displacements

Joint displacement PSD is attained from modal PSD in the following way:

$$[S\delta(n)]_{mxn} = [H^*(n)][S\emptyset(n)][H(n)]$$

where H(n) is a diagonal matrix containing the complex frequency response functions of the various modes considered, and H*(n) is its complex conjugate.
The expression of the frequency responses is:

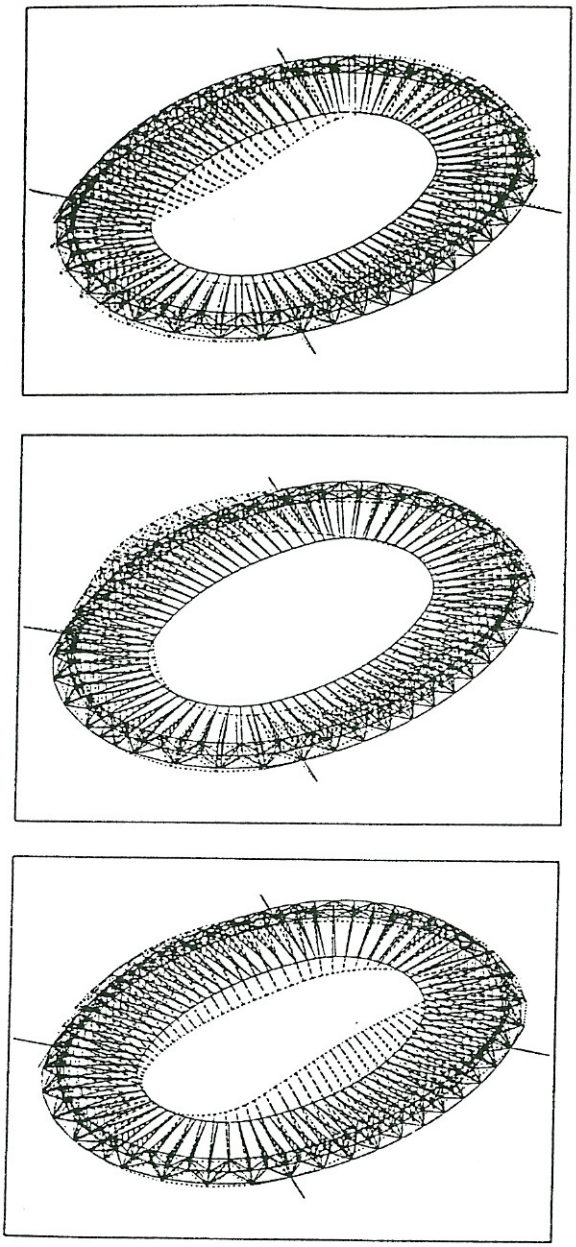

Fig. 7. Axonometric view: mode shape 1-2-3.

$$H(\Omega) = 1/\{K_m[K_m[1+2\ i\lambda_m(n/nm) - (n/nm)^2]\}$$

$$H^*(-i\Omega) = 1/\{K_m[1-2\ i\lambda_m(n/mm) - (n/nm)^2]\}$$

Generalized response-displacements-stresses

The generalized response of the displacements is obtained by passing from mxm rank of the global degrees of freedom 3Nx3N. Thus, for real displacements:

$$[S_G(n)] = [\emptyset][S_g(n)][\emptyset]^T$$

where all of the modes are included in $[\emptyset]$.
The generalized response to stresses in a generic number of elements is obtained by carrying out the following matrix calculation:

$$[S_M\ e(n)] = [K_e][S_g(n)]^*\ [K_e]^T$$

in which $[S_G(n)]^*$ is an elementary submatrix of $[S_G(n)]$.

Maximums of the dynamic response

The hypothesis that pressure fluctuations are considered to be a stationary, Gaussian random process, means that they may also be treated as such in the response process.
Known the power spectral density matrix $[S_G(n)]$ of the movement components, the statistical quantities relating to the latter are assessed as follows:

- standard deviation:

$$\sigma_{Gi} = \{\int_0^{+\infty} S_{Gii}(n)\ dn\]\ ;$$

- peak factor:

$$g_{Gi} = \sqrt{2}\ \ln(\nu_{Gi}T) + 0.5772/\sqrt{2}\ \ln(\nu_{Gi}T)$$

where T = 10 min, the conventional duration of wind action on the roof; ν_{Gi} is the "expected frequency" of the response process, equal to:

$$\nu_{Gi} = [\int_0^{+\infty} n^2\ S_{Gii}(n)dn]/\int_0^{+\infty} S_{Gii}(n)dn$$

and the fluctuating part of the average probable displacements is given by:

$$\{G\}_{fi} = \pm\ g_{Gi}\ \sigma_{Gi}\ .$$

The average value of the dynamic maximums for DT = 10 min, plus the statical response relating to average pressure, gives the check for the effective state.

Use of experimental spectra

As analytical expression for the experimental wind (generalized pressures) spectra are not known the following approximation was felt to be justified: considering the descending branch of the experimental curve relating to the structure's mechanical domain, a curve of the following type, approximating this branch, was drawn:

$$y = a\ x^b\ ,$$

where x is the frequency variable and a and b are the numerical coefficients which define the line of approximation in (bi) logarithmic coordinates. For example, if we take the wind entry angle to be 0°, the spectra related to the frequency range of 0.1-1.0 Hz will be replaced by the following curve:

$$f \times S(n) = 330 \times 10^{-6}\ f^{-1.60}\ .$$

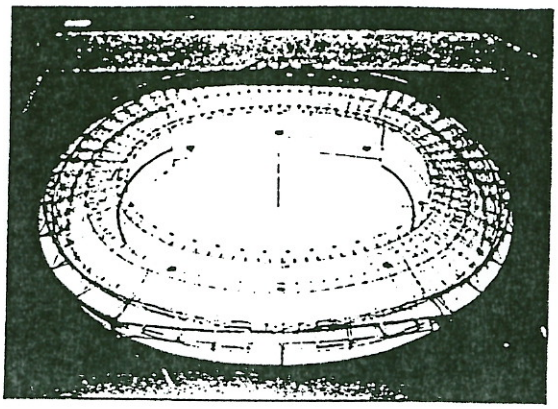

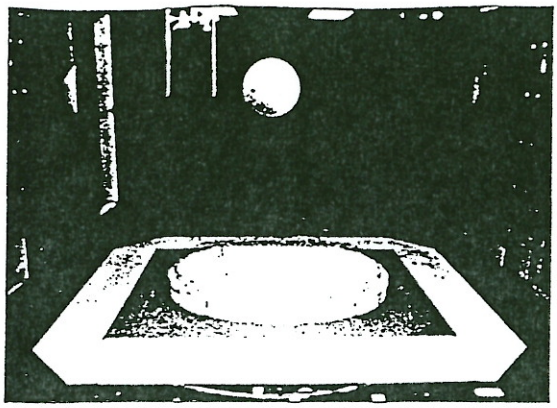

Figs 8 and 9. The aeroelastic model during experimental research in the Wind Tunnel at Western Ontario University (Canada).

nalogous considerations hold true for the area between 0.01 and 0.1 Hz. All of the spectra are given minus a multiplicative constant which is equal to $(1/2\ \rho V)^2$.
There are 30 experimental spectra. Therefore, if we consider wind entry at 0° once more, there are 15 spectra on the part of the roofing below the x-x axis, and another 15 above the axis, but relative to a 180° angle of entry. The whole roof was divided up into 78 panels. For panels without data, interpolation was carried out with adjacent panels.

Experimental check of generalized forces PSD

It is a known fact that the theoretical model of random analysis in the frequency domain has various limitations with regard to definition of wind action on structures. In fact, owing to considerable numerical complications, it is impossible to consider W(t) action perpendicular to wind direction, if in the case of sub-horizontal structures it is still of some importance. Furthermore, the coherence function that may be found in technical literature does not seem to be practical for particularly wide-spanning roofing.
In order to avoid the problems mentioned above an appropriate experimental survey was requested (figs 8 and 9), which has been held in the wind tunnel laboratory of Western Ontario University.
The experimental functions of PSD and coherence were represented on diagrams for 8 sectors of the roof. The processed data was used for the dynamic analysis. In fig. 10 the theoretical and experimental PSD may be compared for a typical roofing panel.

Results of the dynamic analysis

From the comparison of the ESDU spectrum and experimental spectra, we may deduce that: the former has a peak - wind speed function - which is located at 0.05 Hz in our case, and that the latter have a peak at 0.1 Hz.
The ESDU spectrum graph, given in fig. 11, is shown already multiplied by the exponential correlation function coh (P1, P2, f), where P1 and P2 are joints belonging to the same roofing panel.
The decay coefficients were assumed as equal to 2 and 16 with the aim of showing greater damping of correlation in a perpendicular direction along wind direction.
The numerical results of the dynamic analysis and spectra relating to this show that, in the case of the roof in question, the dynamic effects of the wind fundamentally produce pseudostatic type pressures. In other words, almost all of the energy produced by the wind is consumed far from the structure's area of mechanical functioning. This is also confirmed by spectra provided empirically concerning the aeroelastic model.
For vertical displacement of joint 1 (equivalent to site 5 defined by experimenters) the numerical results give a variance value of 0.033 m which, multiplied by the peak factor of 3.51, gives a value of the fluctuating part of the displacement equal to 0.116 m.

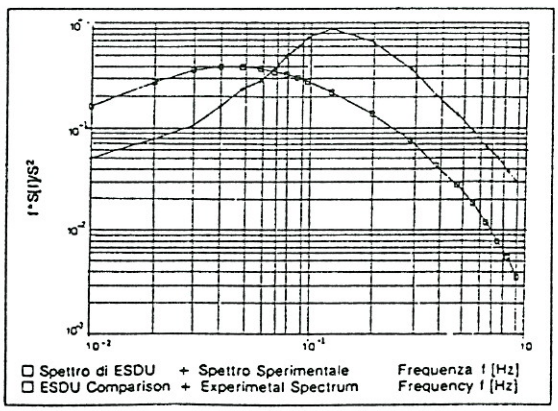

Fig. 10. Comparison between theoretic and experimental wind spectra.

The response spectra given, attained through the dynamic analysis, is shifted from the experimental spectra, especially in the 0.1÷1.0 Hz range. This is due to the fact that, in our survey, we neglected the aerodynamic damping function, regardless of frequency.
Displacement and stress response spectra in important parts of the structure have been represented in diagrams (figs 11 and 12).

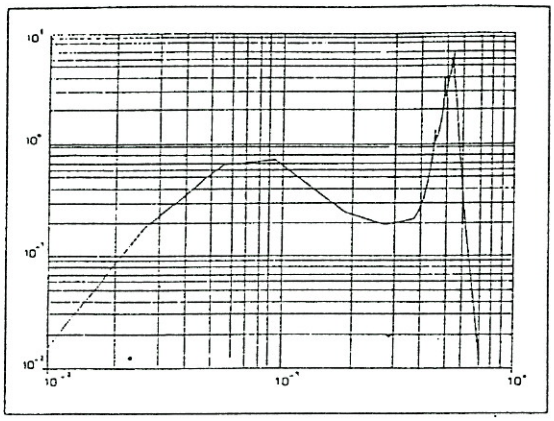

Fig. 11. Vertical displacement response of joint 1.

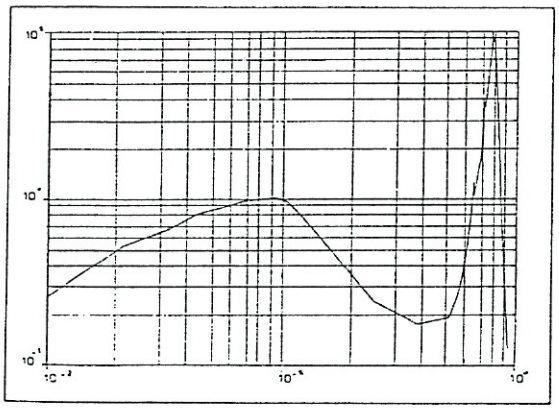

Fig. 12. Response spectrum of tension forces of load-bearing cables.

Mode	Eigenvalue	Frequency	Period
1	9.79224783e+00	3.12925675e+00	2.007884
2	1.17491108e+01	3.42769760e+00	1.833063
3	1.34743432e+01	3.67074151e+00	1.711694
4	1.41655563e+01	3.76371575e+00	1.669410
5	1.77308570e+01	4.21080242e+00	1.492159
6	1.77308570e+01	4.21080242e+00	1.492159
7	2.21803711e+01	4.70960413e+00	1.334122
8	2.41319230e+01	4.91242357e+00	1.279039
9	2.61072114e+01	5.10952165e+00	1.229701
10	2.75590618e+01	5.24967254e+00	1.196872

Geometrical and structrural specifications

Space framed ring

- Max extension of edge structure 870 m.
- Transverse section: irregular triangel.
- Section dimensions along axes:
  base 12.50 m, height 10.50 m.
- Dimensions of tubular joists:
  upper: Ø 1400 mm, thickness 60 to 70 mm;
  lower: Ø 1000 mm, thickness 16 to 18 mm.
- Dimensions of connecting shafts:
  uprights and diagonal braces Ø 409 to 609 mm thickness 8 to 10 mm.
- Joint connecting and stiffening plates: various thicknesses up to 30 mm (figs. 13-14).
- Steel support columns (no. 12):
  height 24 m; Ø 2000 mm; thickness 40 mm.
- Total weight of ring: approx. 50000 KN.

Cable structure

- Max. extension of the central ring: 530 m.
- Number and type of ring cables: 12 Ø 87 mm.
- Radial cable trusses:
  span approx. 46 m; flat type, with load-bearing, stabilizing and connecting cables; cable dimensions (depending on the various state of stress between areas with greater or lesser curvatures): load-bearing Ø 64 or Ø 87 mm; stabilizing Ø 47 or Ø 74 mm; connecting Ø 19 mm.
- Types of terminal cable connection:
  threated cylindrical cable terminal with cast zinc head on adjustable external joints, complete with nut and spherical washer; open bridge socket type cable terminal with pin on the inner ring joints.
- Maximum force applied to the inner tension ring: approx. 50.000 kN.

Covering pre-stressed membrane system

The covering system mainly consistes of two types of elements.

- Radial elements, with plan dimensions of approx. 46x70 m, consisting of panels measuring approx. 5x10 m, which were prefabricated and welded in the workshop, following the cutting pattern worked out through calculation in order to attain typical surfaces with negative Gaussian curvature for the prestressed membranes.
- Cone-shaped elements located inside the external reticular ring, with plan dimensions of 10x12 m, height 6 m, which were also prefabricated in the workshop. The special chimney-like shape of the roofing solution tends to improve microclimatic conditions inside the stadium, with better natural ventilation for spectators seated near to the covering.

The membrane covering is made of a strong fiberglass fabric with an orthotropic weave, covered on both side with PTFE (polytetrafluoroethylene).

Tests carried out on the covering material in laboratories in Italy and the USA gave results which more than satisfied technical specification values. The main results were as follows:

	Test results (birdair)	Specification values
Strip tensile		
Warp	7708 N/5 cm	5430 N/5 cm
Fill	7218 N/5 cm	4200 N/5 cm
Flex fold		
Warp	7393 N/5 cm	4380 N/5 cm
Fill	5556 N/5 cm	3290 N/5 cm

Tensioning of the cable-truss system

The tensioning stage was planned following the same methods used for the lifting operation, i.e. all of the intermediate geometrical and tensile states of the whole structure (structural steel ring/cable trusses/cable ring) were analytically simulated before and then checked during the operation.

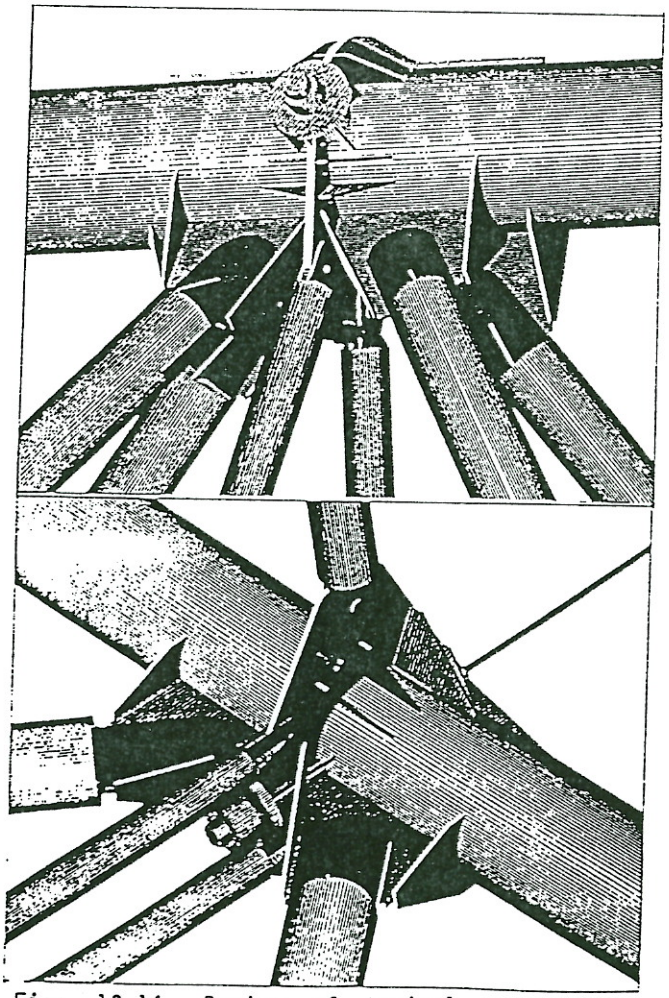

Figs 13-14. Design of typical ring nodes obtained with CAD graphics system.

Positioning of 8 drawing teams at 8 symmetrically distributed points around the structural steel ring (load-bearing and stabilizing cables).
Organization of a central control unit with a radio station and topographical instruments located in the centre of the playing area.
Gradual tensioning, working alternately on the load-bearing then stabilizing cables, with clockwis movement of the work teams from one position to the next. The teams worked their way completely around the fing three times.
The upper jacks were of a perforated type, with a 300 t capacity, used singly, while the lowere ones were rod-type with a 250 t capacity, used in pair.

Geometrical and pre-stressing control

This check involved measurement of the structure's geometrical characteristics and strain in the cable and ring system, and on line comparison with the values obtained through structural analysis.

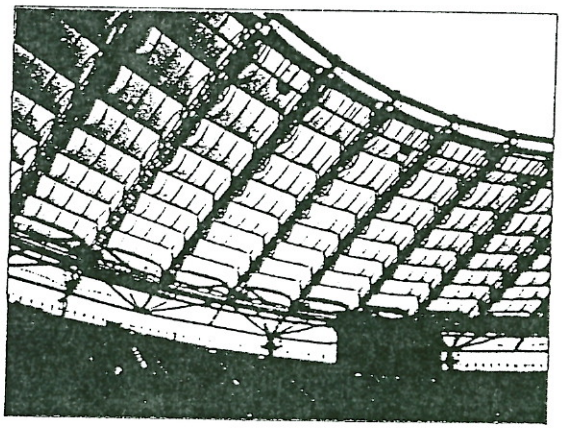

Fig. 15. Internal view of the 55 m cantilever membrane covering.

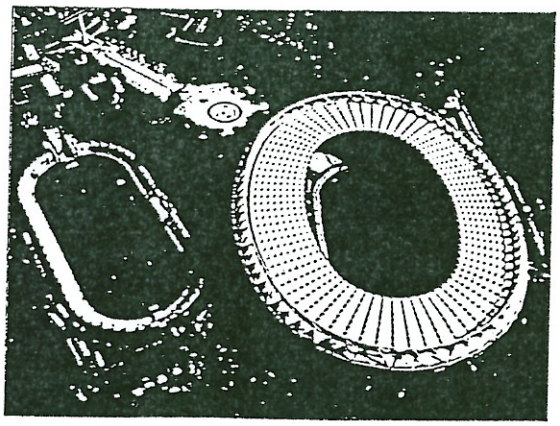

Fig. 16. Aereal view of the completed roofing.